Lighting the Universe with filaments

Liang Gao[1,*], Tom Theuns[1,2]

1 Institute for Computational Cosmology, Durham University, South Road, Durham DH1 3LE, UK

2 Department of Physics, University of Antwerp, Groenenborgerlaan 171, B-2020 Antwerpen, Belgium

* E-mail: liang.gao@durham.ac.uk

The first stars in the Universe form when chemically pristine gas heats as it falls into dark matter potential wells, cools radiatively due to the formation of molecular hydrogen, and becomes self-gravitating. We demonstrate with super-computer simulations that their properties depend critically on the currently unknown nature of the dark matter. If the dark matter particles have intrinsic velocities that wipe-out small-scale structure, then the first stars form in filaments with lengths of order the free-streaming scale, which can be $\sim 10^{20}$ m (~ 3 kpc, baryonic masses $\sim 10^7$ solar masses) for realistic 'warm dark matter' candidates. Fragmentation of the filaments forms stars with a range of masses which may explain the observed peculiar element abundance pattern of extremely metal-poor stars, while coalescence of fragments and stars during the filament's ultimate collapse may seed the super massive black holes that lurk in the centres of most massive galaxies.

Most of the matter in the Universe does not interact with light except gravitationally. This 'dark matter' is usually assumed to be 'cold', meaning that its velocity dispersion is sufficiently small for density perturbations imprinted in the early Universe to persist up to very small scales. Although this model is able to describe the large-scale distribution of galaxies in impressive detail, it may face problems on the scale of galaxies and below, for example it may predict too many satellite galaxies ([1]), as well as too cuspy profiles for the dark matter halos that surround galaxies ([2]).

However, dark matter has yet to be detected in the laboratory, and there exist many viable dark matter candidates from particle physics that are not 'cold' . Warm dark matter (WDM) particles have intrinsic thermal velocities and these motions quench the growth of structure below a 'free-streaming' scale (the distance over which a typical WDM particle travels) which depends on

the nature of the particle. Because small and dense halos do not form below the free-streaming-scale, the dark matter halos that surround galaxies in a WDM model have far less substructure and are less concentrated as compared to their cold dark matter (CDM) counterparts, which may help alleviate both the satellite and galactic core problem (*3*). Structures on larger scales are similar in WDM and CDM and therefore the distribution of galaxies is not affected. The first generation of stars in the Universe forms when primordial gas gets compressed by falling into small dark matter potential wells (*4–7*). Because WDM affects structure formation on such small scales it may influence how the first stars form; we have performed simulations to analyse this in more detail.

Large-scale power in the spectrum of density perturbations causes progenitors of present-day clusters of galaxies to be amongst the first objects to condense out of the initially almost smooth mass distribution. We study the early formation stages of such an object by identifying a massive cluster of galaxies in a dark matter simulation of a large cosmological volume at redshift $z = 0$, and use a multi-scale technique (*8, 9*) to re-simulate its formation and evolution with the cosmological hydrodynamics code Gadget-2 (*9, 10*). Baryons compressed by falling into the developing dark matter potential wells cool radiatively through molecular hydrogen emission lines (*9, 11*); we follow the formation of molecular hydrogen and its cooling using a sophisticated chemistry network (*6*). The parent simulation, from which we picked the re-simulated region, followed the growth of structure in a CDM dominated Universe with a cosmological constant Λ (ΛCDM); we performed the re-simulations assuming both CDM and WDM as dark matter. In this WDM model, small scale power in the density fluctuations is exponentially suppressed below ~ 100 co-moving kpc, mimicking free-streaming of gravitino particles with mass $m_{\mathrm{WDM}} = 3\,\mathrm{keV}$ (*3*). Gravitinos are a popular WDM candidate (*12*) but our results are insensitive to the exact choice of WDM particle as long as its free-streaming length is more than a few tens of co-moving kilo parsecs. Therefore even if the gravitino were slightly more massive, or if the WDM were instead a sterile neutrino (another popular WDM candidate (*13*)), our results would not change appreciably. Observations of the clustering of neutral gas along sight lines to distant quasars (the Lyman-α forest of absorption lines) probe scales $1 - 40$ Mpc when the density perturbations on these scales are still small, and the presence or absence of significant substructure in these observations can constrain the masses of WDM particles (*14, 15*); our choice of WDM particle mass (3 keV, the corresponding mass-scale is $\sim 3 \times 10^8 M_\odot$) is well above this lower limit (~ 2 keV; 14, 15). The initial amplitude of the imposed density perturbations in our simulations is normalised to the level seen in the Cosmic Microwave Background radiation (*16*), and our simulations start at redshift $z \sim 200$. (See the supplementary online material for more details on these simulations.)

The growth of structure in these re-simulations leads to a pattern of filaments and sheets (Fig.1) familiar from the local large-scale distribution of galaxies. This is because the assumed Gaussian spectrum of density perturbations, appropriate for an inflationary model, leads to collapse along one (sheet) and two directions (filament) before the formation of halos. Although the large-scale filamentary pattern is very similar in CDM and WDM, the structure of the filaments themselves is very different: whereas the CDM filaments fragment into numerous nearly

spherical high density regions ('halos'; panel 1.a), the WDM filaments are mostly devoid of such substructure (panel 1.b). Panels 1.c and 1.d depict the WDM filament at an earlier time before any of the other filaments have formed: the central density is very high (hydrogen number density $n_{\rm h} \sim 10^4\,{\rm cm}^{-3} \approx 10^6 \langle n_{\rm h} \rangle$) yet no dark matter halo has formed yet. It is well known that the Poisson noise in simulation codes that use particles to represent the dark matter leads to spurious fragmentation of the filaments that form in such WDM simulations ([17, 18]). We therefore end the analysis of our WDM simulations well before filaments fragment.

The length of the filament ($\sim$ 3 kpc) is of order of the imposed WDM free-streaming scale as expected, $L \sim 4$ kpc at redshift $z = 23.34$ when the Universe is 140 million years old. Gas and dark matter accrete perpendicular onto the filament's axis (Fig. 2). Dark matter particles falling into the filament perform damped oscillations as the potential well deepens. At $r \sim 50$ pc (where r is the distance perpendicular to the filament's axis) dark matter particles falling into the well encounter particles that fell in from the other side, and such successive instances of 'orbit-crossing' give rise to the steps in the density seen in Fig. 1b. Baryons do not undergo orbit-crossing but the gas gets compressed to a temperature $T \approx 7000$ K at $r \sim 20$ pc. Rapid build-up of H_2 induces cooling and the gas starts to dominate the matter density further downstream, so that the ratio of gas to dark matter densities $\rho_b/\rho_{\rm DM} \sim 15 = 100 \langle \rho_{\rm b} \rangle / \langle \rho_{\rm DM} \rangle$ at $r = 2$ pc. At $r < 2$ pc where the gas dominates, the ratios of principal axes of the filament are $b/a = 0.123$ and $c/a = 0.118$ hence the filament is very nearly cylindrical. The properties of both the gas and the dark matter are very uniform along the whole length of the filament. The cylindrical density profile below 10 pc is approximately $\rho \propto r^{-2.8}$ for $2 \leq r \leq 8$ pc and $\rho \propto r^{-2}$ for $r < 2$ pc. This contrasts with $\rho \propto r^{-2.3}$ for the spherically averaged profile of the gas in CDM halos on a comparable scale ([6, 7]). The central H_2 abundance reaches 10^{-3}, higher than in the CDM case because of the higher temperature reached behind the accretion shock. This higher temperature, and the associated higher ionisation fraction, will also enhance the importance of HD cooling at later stages ([19, 20]).

The non-linear collapse into a thin filament found in these WDM simulations is in sharp contrast to what happens in the CDM case. There the first objects to reach high densities are discrete, nearly spherical, dark matter halos (gravitationally bound concentrations of dark matter) that form at tiny masses and build-up hierarchically through mergers and accretion. Some halos have a sufficiently deep potential well to accrete and shock baryons, enabling H_2 formation and radiative cooling. Runaway collapse of the rapidly accreting self-gravitating gas is thought to lead to the formation of a single massive star per cooling halo ([4, 6, 7]). The absence of small scale power in WDM prevents halos from forming before the filament itself becomes highly non-linear. Although our re-simulations focus on the progenitor of a massive cluster, and hence the forming object collapses unusually early on, the fact that very high densities are reached in a filament, as opposed to a spherical halo, is generic to WDM.

The stability of collapsing filamentary clouds has been investigated in the context of the formation of cloud cores by for example ([21, 22]), and applied to early Universe filaments ([23]). The inability of gas to cool sufficiently fast usually limits the collapse time of the filament by the cooling time, $t_d \equiv \rho/\dot{\rho} \sim t_c \equiv n k_{\rm Boltz} T / \Lambda$ (where T is the temperature and Λ is the cooling

rate due to H_2 and HD cooling). Perturbations start growing, possibly leading to fragmentation, when the dynamical time $t_d \gg t_p$, where t_p is the inverse growth rate of perturbations. If gas cooling is efficient, $t_d \sim t_c \ll t_p$, and perturbations do not grow. At densities $n = n_1 \sim 10^5$ cm^{-3} the level population of H_2 reaches LTE making $\Lambda \propto n$ instead of $\propto n^2$ and t_d increases (*11*). A sufficiently massive filament may yet survive fragmentation at this stage, and at higher density $n \sim 10^9$ cm^{-3} three-body processes promote the formation of H_2 and the cooling time decreases again. However when $n \geq n_2 = 10^{12}$ cm^{-3} the gas becomes optically thick in the H_2 cooling transitions slowing the collapse and the filament is once more in danger of fragmenting. Collision induced continuum emission will again decrease the cooling time when $n \sim 10^{14}$ cm^{-3}, until the gas becomes optically thick also to this cooling radiation at densities $n \geq n_3 = 10^{16}$ cm^{-3} (*20, 24*). The physics of the H_2 molecule therefore sets three densities at which the filament may fragment. The typical fragment masses are of order tens of solar masses, solar masses, and sub-solar masses, for fragmentation at densities n_1, n_2 and n_3, respectively (*23*).

The tidal field around the filament breaks the cylindrical symmetry on scales comparable to the filament's length (Fig. 1), and can trigger the gas dynamical instabilities that ultimately lead to fragmentation. Unfortunately our current simulations are not able to follow this process in detail because these tiny deviations from symmetry are overpowered by numerical noise caused by the graininess of the particle distribution. This causes the filament to fragment very rapidly as expected, yet the scale of the fragmentation is artificial. In the WDM universe, the small-scale perturbations that trigger fragmentation in the simulations are not present and need to be generated through transfer of power from larger scales. Since this is a relatively slow process, the central density will have reached the higher value n_2 or even higher, implying small fragment masses of order of a solar mass or below. Such fragments can coalesce to form more massive clumps, as demonstrated in 2D numerical simulations (*22*). Even if individual cores survive, they may still grow in mass through accretion.

Detailed observations of star-forming clouds in the Milky Way reveal that the low-mass stellar mass function is very similar to that of the dense, pre-stellar cloud cores within the ambient cloud, although it is not yet clear what determines the cut-off at high masses. This close similarity might indicate that the process of cloud fragmentation plays an important role in determining the initial mass function (*25*). If this also applies to star-formation in a WDM filament, then it is plausible that fragmentation will lead to a burst of star formation which includes low-mass stars with masses $\sim 1~M_\odot$ or below, but also much more massive stars built through mergers and accretion. The more massive stars will end their short lives through supernova explosions or collapse to form intermediate mass black holes, and some of the very low mass stars may potentially survive until today. Although the details of this scenario are uncertain, it is clear that the stellar mass function will be quite different from the CDM case.

The low-mass Milky Way stars HE 0107-5240 (*26*) and HE 1327-2326 (*27*) have extremely low metallicities[1] of [Fe/H] ~ -5 and peculiar element abundances, for example [C/Fe]>1. An

---

[1]The notation [X] $\equiv$ log(X/X$_0$), characterises the mass fraction of element X in terms of the value in the Sun, X$_0$.

initial mass function of zero metallicity first stars with a range of masses, as we suggested might be the case in WDM, could explain these stars either as due to self-pollution or pre-enrichment by intermediate mass (tens of solar masses) supernovae (*28*). Such first generation low and intermediate mass stars are not thought to form in CDM (*4, 6, 7*). Therefore, although the present observational evidence is not yet unambiguous, a future detection of zero-metallicity low-mass first stars may indicate that the dark matter is warm.

Free-streaming of the WDM decreases significantly the number density of halos that host early star formation, which could delay reionization as compared to CDM (*29*). However the additional mode of star formation in filaments could partly compensate, making it unclear whether reionization is indeed delayed when the dark matter is warm.

What is the ultimate fate of such $\sim 10^7 \, M_\odot$ filaments? Eventually the filament will collapse along its long axis, and since its mean density is very high a significant number of collisions between cloud cores and stars would appear inevitable. Such collisions could build-up a massive object which can seed the formation of the super-massive black holes that power redshift $z \sim 6$ quasars, and appear to lurk in the centers of most large galaxies today.

The different outcome of WDM versus CDM is because the thermal velocities of the WDM particles prevent halos from forming before the filaments themselves form stars. This happens when the free-streaming length introduced by the dark matter's thermal velocities is more than a few tens of co-moving kilo parsecs so that the filaments are sufficiently massive to heat infalling gas to more than ~1000 K, enabling efficient cooling by molecular hydrogen. If we simulate a WDM Universe with much shorter free-streaming length, for example ~ 20 kpc corresponding to a gravitino mass $m_{WDM} = 15$ keV, star formation proceeds in a similar way to the CDM case, in good agreement with earlier work (*30*). The likely very different initial mass function of the first stars and the rapid formation of massive black holes in a WDM scenario with $m_{WDM} \sim$ 3 keV, as opposed to CDM, implies a very different early thermal and metal enrichment history of the Universe, greatly affecting subsequent galaxy formation. It appears therefore that the way in which quasar, star and galaxy formation started, depends strongly on the nature of the dark matter.

References and Notes

1. B. Moore, S. Ghigna, F. Governato, G. Lake, T. Quinn T., J. Stadel, P. Tozzi, *The Astrophys. J.*, **524**, L19 (1999)

2. J. J. Dalcanton, C. J. Hogan, *The Astrophys. J.*, **561**, 35 (2001)

3. P. Bode, J. P. Ostriker, N. Turok, *The Astrophys. J.*,**556**, 93 (2001)

4. T. Abel, G. L. Bryan, M. L. Norman,*Science*, **295**, 93 (2002)

5. V. Bromm, P. S. Coppi & R. B. Larson, *The Astrophys. J.*, **564**, 23 (2002)

6. N. Yoshida, K. Omukai, L. Hernguist,T. Abel, *The Astrophys. J.*, **652**, 6 (2006)

7. L. Gao, N. Yoshida, T. Abel, C. S. Frenk, A. Jenkins, V. Springel, *Mon. Not. R. Astron. Soc.*, **378**, 449 (2007)

8. Gao L., White S. D. M., Jenkins A., Frenk C. S., Springel V., *Mon. Not. R. Astron. Soc.*, **363**, 379 (2005)

9. See supporting material on Science on line.

10. V. Springel, *Mon. Not. R. Astron. Soc.*, **364**, 1105 (2005)

11. D. Galli, F. Palla, *Astron. & Astrophys.*, **335**, 403 (1998)

12. G. Bertone, D. Hooper, J. Silk, Particle dark matter: evidence, candidates and constraints, *Physics Report*, **405**, 279 (2005)

13. S. Dodelson, L. M. Widrow, *Phys. Rev. Lett.*, **72**, 17 (1994)

14. M. Viel, J. Lesgourgues, M. G. Haehnelt, S. Matarrese, A. Riotto, *Phys. Rev. Lett.*, **97**, 071301 (2006)

15. U. Seljak., A. Makarov, P. McDonald, H. Trac, *Phys. Rev. Lett.*,**97**, 191303 (2006)

16. D. N. Spergel *et al.*, *The Astrophys. J.* in press, preprint astro-ph/0603449 (2007)

17. M. Götz, J. Sommer-Larsen, *Astron. & S. Sci.*, **281**, 415 (2002)

18. J. Wang, S. D. M. White, preprint, astro-ph/0702575 (2007)

19. Johnson, J. L., & Bromm, V., *Mon. Not. R. Astron. Soc.*, **366**, 247 (2006)

20. Yoshida, N., Oh, S. P., Kitayama, T., Hernquist, L., *The Astrophys. J.*, **663**, 687 (2007)

21. R. B. Larson, *Mon. Not. R. Astron. Soc.*, **214**, 379 (1985)

22. S. Inutsuka, S. M. Miyama, *The Astrophys. J.*, **480**, 681 (1997)

23. F. Nakamura, M. Umemura, *The Astrophys. J.*, **569**, 549 (2002)

24. Omukai, K., Nishi, R., *The Astrophys. J.*, **508**, 141 (1998)

25. Larson, R. B., *Mon. Not. R. Astron. Soc.*, **359**, 211 (2005)

26. N. Christlieb, M. S. Bessell, T. C. Beers, B. Gustafsson, A. Korn, P. S. Barklem, T. Karlsson, M. Mizuno-Wiedner, S. Rossi, *Nature*, **419**, 904 (2002)

27. Frebel *et al.*, *Nature*, **434**, 871 (2005)

28. Beers T. C., Christlieb N., *Annu. Rev. Astron. Astrophys.*, **43**, 531 (2005)

29. Yoshida N., Sokasian A., Hernquist L., Springe V., *The Astrophys. J.*, **591**, 1 (2003)

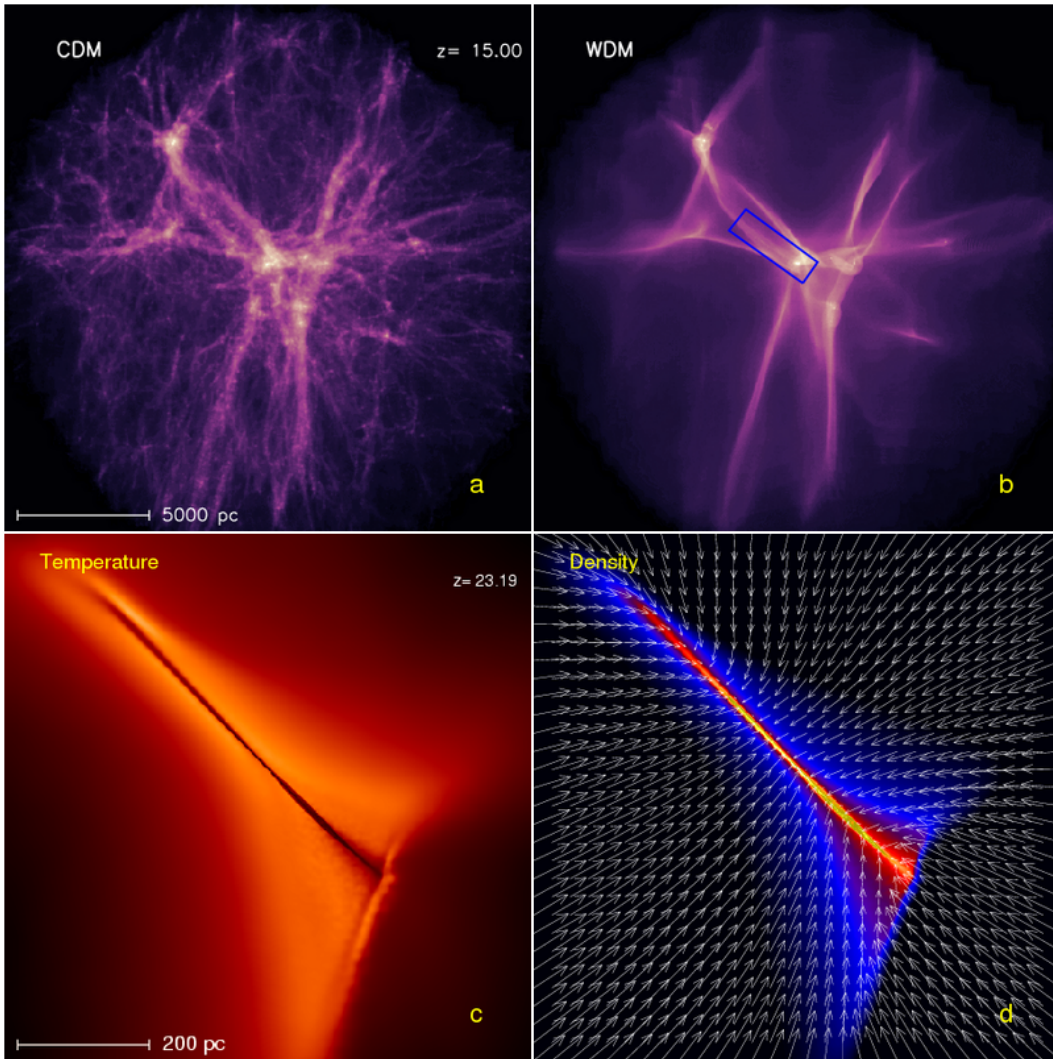30. O'Shea B. W., Norman, M. L. , *The Astrophys. J.*, **648**, 31 (2006)

Figure 1

Top panels: Dark matter density structure of the progenitor of a redshift $z = 0$ massive cluster of galaxies at $z = 15$ when the thermal velocities of the dark matter particles are negligible (CDM; panel a) and when the dark matter is 'warm' (WDM; a gravitino with $m_{\mathrm{WDM}} = 3$ keV; panel b). Although both models produce a characteristic filamentary pattern in the density, the CDM filaments fragment into numerous nearly spherical halos whereas free-streaming of the WDM prevents such substructure from forming. *Bottom panels:* Gas temperature (panel c) and density (panel d) in the WDM filament indicated by the red box in panel b, at an earlier redshift ($z = 23.34$) when only this filament had formed. Gas accretes very uniformly onto the filament as indicated by the velocity vectors, heats as it gets compressed, but further downstream cools due to the formation of H_2, making the centre of the filament cold and dense. The filament shown here is almost perfectly cylindrical, more generally they are elliptical in shape.
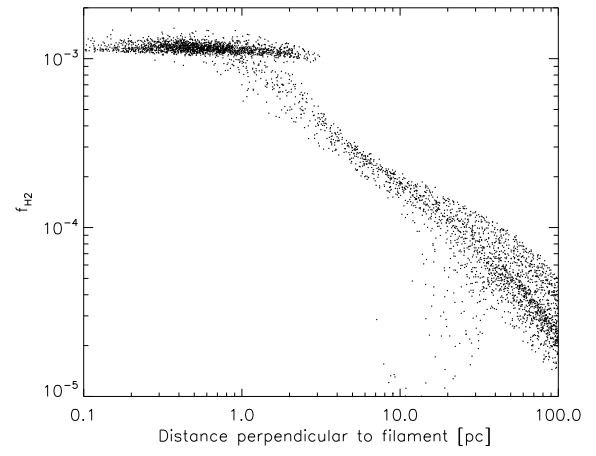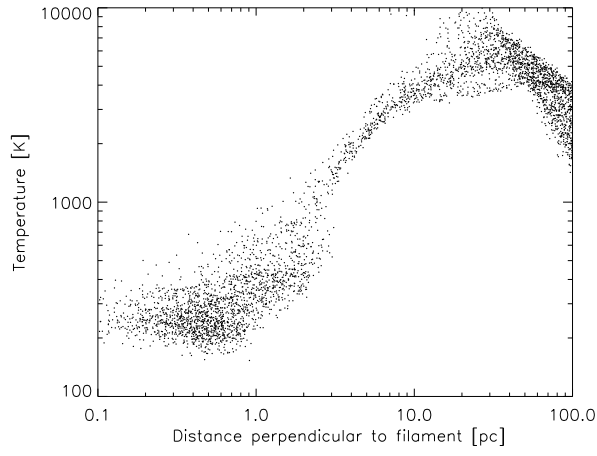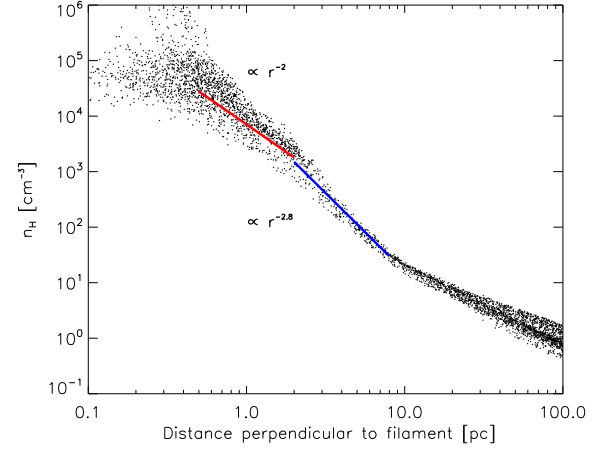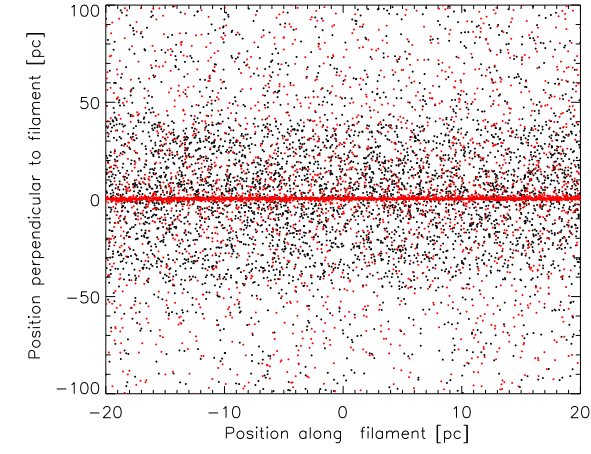
Figure 2

Gas and dark matter profiles of the WDM filament shown in panels c and d of Fig. 1. Top left: accretion of dark matter particles (black) and gas particles (red); note the different horizontal and vertical scales (along and perpendicular to the filament, respectively). The dark matter undergoes orbit-crossing (multi-valued velocities) at $r \sim 50$ pc, whereas the gas gets shocked much closer in (~ 20 pc) and dominates further downstream. Top right: gas density profile as measured perpendicular to the filament's axis. Lines $\rho \propto r^{-2}$ and $\rho \propto r^{-2.8}$ are drawn to guide the eye. Bottom left: temperature profile: gas heats as it gets compressed, but the rapid build-up of H_2 cools the gas further in. Bottom right: Build-up of molecular hydrogen fraction, f_{H_2}, during the accretion.

Supporting Online Material
Material and Methods
SOM text
Figs:S1

SUPPORTING ONLINE MATERIAL

We briefly describe the setup of the initial conditions, how we model the effect of warm dark matter, the chemistry network, and the numerical method used.

1 Numerical Methods

1.1 Cosmological initial conditions

The theory of inflation posits that quantum mechanical fluctuations in the 'inflaton' field were blown-up to macroscopic scales during a short period of rapid expansion called inflation. These small perturbations in the density have grown due to gravity into the large-scale structure we see today (*S1*). The initial conditions of a cosmological simulation represent these initially small perturbations at the starting redshift of the simulation in a periodic, computational box of given co-moving size. The simulation then follows how these small ripples develop into high and low-density regions.

If the statistics of the perturbations are those of a Gaussian field, as is thought to be the case in inflation, then the initial fluctuations are fully described by their power-spectrum, $P(k, t)$, which characterises the amplitude of the fluctuations as function of scale, $\lambda = 2\pi/k$, at time t. The Warm Dark Matter (WDM) and Cold Dark Matter (CDM) power spectra from *(S2)* are plotted in Fig. S1: free-streaming of a WDM particle with mass $m_{WDM} = 3$ keV suppresses power below a scale ~ 100 kpc as compared to CDM.

Setting-up initial conditions now boils down to generating a Gaussian field with known power-spectrum, which is done using Fourier transform methods. Since our simulation code uses particles to represent the matter distribution, we need to generate a particle distribution to represent this density field. We start by creating a homogeneous particle distribution, either by simply putting equal mass particles on the vertices of a regular grid, or as done here, starting from a glass distribution. We then use the Zel'dovich approximation (*S3*) to displace these particles to represent the density field (see also *S4*). The physical power-spectrum has power on all scales, but the particle distribution cannot represent waves larger than the box size, or smaller than twice the inter particle spacing d.

The dark matter structures that host the very first stars are very rare objects, therefore cosmological simulations of such early structure formation must model extremely large volumes in order to sample these rare objects. However, the simulations must also achieve very high mass resolution to follow accurately how gas collapses to high densities in these early potential wells. The contradictory requirements of large simulation volume yet high resolution make cosmological simulation of these structures unfeasible with uniform mass resolution given current computational resources. Therefore we use a 'multi-scale re-simulation technique' to overcome this dilemma. In a re-simulation, only a sub-volume of the whole simulation volume (containing the object in which we are interested) is simulated with very high resolution, while the rest

of the computational domain is sampled at much coarser resolution. The advantage is that it enables us to obtain the extremely high dynamic range in mass and length required for the current problem; the challenge is how to generate the appropriate initial conditions (ICs).

We begin by generating ICs in a large periodic box (479 Mpc, the 'parent simulation') as described above, and evolve the system forward in time using Gadget-2 (see *S5)*, following just the growth of structure in the dark matter for simplicity and speed. Once this simulation reaches redshift $z = 0$, we analyse it and search for a massive dark matter halo, such as would envelope a massive cluster of galaxies (or any other structure of interest).

Next we create a multi-mass particle distribution to represent the unperturbed homogeneous universe, by concentrating lower-mass particles in the region of interest, with successive layers of more massive particles away from this region. The original displacements field for the parent simulation is recreated and the displacements applied everywhere. In the region of interest, the inter particle spacing is smaller, and we can include power on smaller scales than was possible with the original coarser particle distribution. This small scale power is generated by creating a periodic cubic Fourier mesh which is placed around the region of interest. A displacement field is created on this mesh, with the appropriate power spectrum, taking wave numbers between the cut-off in power spectrum of the parent simulation and the Nyquist frequency, $k = \pi/d$, of the region of interest determined by the inter particle spacing, d, there. Typically the longest waves used in the small scale power have a maximum wavelength of a tenth of the cubic Fourier mesh (if the maximum wavelength were to be much larger this procedure would start becoming inaccurate because periodicity is enforced by the method over the mesh). The second set of displacements which represent the additional small scale power, is then applied to the particles inside the high resolution region only. The scheme used to interpolate the displacements to the positions of the particles takes account of the mass of the particles to avoid aliasing effects for the most massive particles in the high resolution region.

Having created these initial conditions and run them forward in time, a new region of interest can be defined for this re-simulation at the same or different redshift, and a re-simulation of the re-simulation can be made following the same procedure where the parent simulation is now identified as the first re-simulation. The simulations described in this paper apply this procedure four times in order to generate ICs for the progenitor of a massive cluster of galaxies at redshift $z = 0$, and its surroundings; see (*S6*) for further details. The main difference here is that we used a WDM power spectrum for generating the initial density field. Note, for simplicity we did not add the thermal velocities of the WDM particles, hence the free-streaming of the WDM is mimicked just by their suppression of small-scale power.

The highest resolution achieved in our final simulation is $M_{dm} = 272.6\, M_\odot$ and $M_{gas} = 41.9\, M_\odot$ for dark matter and gas particles respectively, and the high resolution region has a Lagrangian radius of about 600 comoving kpc.
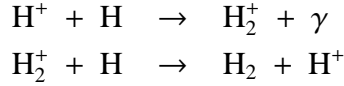
1.2 The simulation code Gadget-2

Gadget-2 (see *S5*) is a Lagrangian code that uses two sets of particles to represent dark matter and gas. Each gas and dark matter particle represents a swarm of baryonic particles and gravitinos, respectively. Because the simulation particles are so much more massive than the physical particles they represent, we soften the gravitational forces between simulation particles to minimise numerical artifacts. Each dark matter particle in the simulation has a position, velocity, (constant) mass, and gravitational softening length. Gas particles have in addition a thermal energy and gas smoothing length, in addition to properties to follow the molecular hydrogen formation (see next section). Gadget-2 uses the smoothed particle hydrodynamics (SPH) scheme to evaluate pressure gradients between particles. Once gravitational and pressure accelerations are computed, the state of system is marched forward in time. Gadget-2 uses a sophisticated tree structure to perform these force calculations efficiently on a parallel computer with message-passing interface (MPI). Full details on Gadget-2 are given in *S5*.
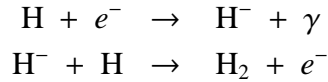
2 Primordial gas chemistry

In this section, we briefly summarise the basic gas processes that are important for primordial gas unpolluted by metals; full details are given in *(S6-10)*.

At high redshifts, in the absence of metals, and when the temperature of gas is lower than 10^4K (above which atomic hydrogen line cooling is dominant), the main coolant enabling star formation in the early dark matter potential wells, is molecular hydrogen, H_2. Its formation has three main channels:
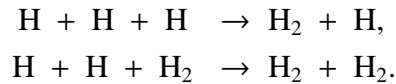
1. the H_2^+ channel

$$H^+ + H \rightarrow H_2^+ + \gamma$$
$$H_2^+ + H \rightarrow H_2 + H^+$$

2. the H^- channel

$$H + e^- \rightarrow H^- + \gamma$$
$$H^- + H \rightarrow H_2 + e^-$$

3. the three-body reaction

$$H + H + H \rightarrow H_2 + H,$$
$$H + H + H_2 \rightarrow H_2 + H_2.$$

The first channel dominates at high redshift, $z \geq 200$, and the three-body reactions are important only at high densities ($n_H \sim 10^8 \text{cm}^{-3}$); therefore the H^- channel is most relevant for the initial

stages in the formation of the filament discussed in this paper. Our simulation code follows reactions for 9 species (e^-, H, H$^+$, He, He$^+$, He^{++}, H$_2$, H$_2^+$, H$^-$), and includes all three H$_2$ formation channels.

References and Notes

S1. P. J. E. Peebles, *Princeton University Press* (1993)

S2. P. Bode, J. P. Ostriker, N. Turok, *The Astrophys. J.*,**556**, 93 (2001)

S3. Y. B. Zel'Dovich, *Astron. & Astrophys.*,**5**, 84 (1970)

S4. G. Efstathiou, M. Davis, S. D. M. White, C. S. Frenk, *The Astrophys. J.*, **57**, 241 (1985)

S5. V. Springel, *Mon. Not. R. Astron. Soc.*, **364**, 1105 (2005)

S6. Gao L., White S. D. M., Jenkins A., Frenk C. S., Springel V., *Mon. Not. R. Astron. Soc.*, **363**, 379 (2005)

S7. F. Palla, E. E. Salpeter, S. W. Stahler, *The Astrophys. J.*, **271**, 632 (1985)

S8. D. Galli, F. Palla, *Astron. & Astrophys.*, **335**, 403 (1998)

S9. N. Yoshida, K. Omukai, L. Hernguist,T. Abel, *The Astrophys. J.*, **652**, 6 (2006)

S10. L. Gao, N. Yoshida, T. Abel, C. S. Frenk, A. Jenkins, V. Springel, *Mon. Not. R. Astron. Soc.*, **378**, 449 (2007)
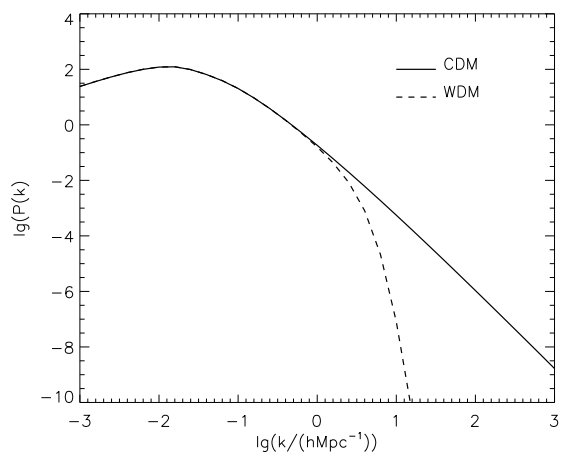
Figure S1
Power-spectrum for CDM (drawn line) and WDM (dashed line). Free-streaming of the warm dark matter particle (a gravitino with mass $m_{\mathrm{WDM}} = 3$ keV) exponentially suppresses power below a scale ~ 100 kpc.